Inactivation of Ribonucleotide Reductase by (*E*)-2′-Fluoromethylene-2′-deoxycytidine 5′-Diphosphate: A Paradigm for Nucleotide Mechanism-Based Inhibitors†

Wilfred A. van der Donk,‡,⊥ Guixue Yu,‡,§,⊥ Domingos J. Silva,⊥ and JoAnne Stubbe*,⊥,▽

Departments of Chemistry and Biology, Massachusetts Institute of Technology, Cambridge, Massachusetts 02139

James R. McCarthy,|| Esa T. Jarvi, Donald P. Matthews, Robert J. Resvick, and Eugene Wagner

Marion Merrell Dow Research Institute, 2110 East Galbraith Rd, Cincinnati, Ohio 45215

Received January 25, 1996; Revised Manuscript Received April 10, 1996⊗

ABSTRACT: Ribonucleotide reductase (RDPR) from *Escherichia coli* catalyzes the conversion of nucleotides to deoxynucleotides and is composed of two homodimeric subunits: R1 and R2. (*E*)- and (*Z*)-2′-fluoromethylene-2′-deoxycytidine 5′-diphosphate (FMCDP) are time dependent inactivators of this protein, with ∼1.5 equiv being sufficient for complete loss of catalytic activity. Inactivation results from loss of the essential tyrosyl radical on R2 and alkylation of R1. Studies using electron spin resonance spectroscopy reveal that tyrosyl radical loss is accompanied by formation of a new, substrate-based radical. Experiments using [6′-^{14}C]-(*E*)-FMCDP and [5-^{3}H]-(*E*)-FMCDP reveal that alkylation of R1 is accompanied by release of 0.5 equiv of cytosine and 1.4 equiv of fluoride ion. When R1 is denatured subsequent to inactivation, ∼1 equiv of label per R1 is observed only in studies carried out with [^{14}C]FMCDP. Under these same conditions with [^{3}H]FMCDP, 1.5 equiv of radiolabel is detected as cytosine. Inactivation of R1 thus results from alkylation by the sugar moiety of FMCDP. While studies to isolate the alkylated amino acid on R1 were unsuccessful, studies using a variety of site-directed mutants of R1 (C462S, C225S, C754/759S, C439S, and E441Q) indicate that E441 or possibly C439 is the modified residue. Inactivation is accompanied by rapid formation of a new chromophore with a λ_{max} at 334 nm. Dithiothreitol does not protect the enzyme against inactivation by FMCDP, although it does prevent chromophore formation. Two possible mechanisms are proposed to accommodate these experimental observations.

Two nucleoside analogs, gemcitabine (2′-deoxy-2′,2′-difluorocytidine) (Grunewald et al., 1990; Abbruzzese et al., 1991) and (*E*)-2′-fluoromethylene-2′-deoxycytidine (E-FMC)[1] (McCarthy et al., 1991; Kanazawa et al., 1995; McCarthy & Sunkara, 1995), have recently been shown to possess potent chemotherapeutic efficacy against leukemias and solid tumors. The cytotoxicity has been proposed to result from the ability of the corresponding triphosphates to function as DNA chain terminators in the DNA polymerase catalyzed elongation reaction (Huang et al., 1991; McCarthy & Sunkara, 1995; R. Snyder, unpublished results). Previous studies by Baker et al. (1991) and the results reported in the present paper, however, indicate that the corresponding diphosphates of these compounds can function as potent mechanism-based inhibitors of ribonucleotide reductases (RNRs), the enzymes that catalyze the conversion of nucleotides to deoxynucleotides, the rate-determining step in DNA biosynthesis. Thus it is likely that inhibition of RNR potentiates the effect of these DNA chain terminators by lowering the deoxynucleoside triphosphate (dNTP) pools, minimizing the competition for incorporation of the chain

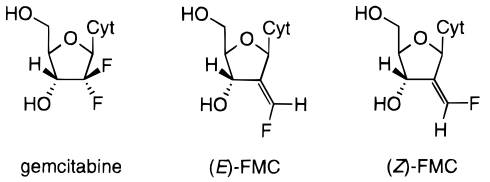

† This research was supported by grants from the National Institutes of Health to J.S. (GM-29595), by a postdoctoral fellowship to W.A.v.d.D. from the Jane Coffin Childs Foundation for Medical Research (Project 61-960), and by a postdoctoral fellowship from the Cancer Research Fund of the Damon Runyon−Walter Winchell Foundation to D.J.S. (DRG-1333).

* Corresponding author.

‡ These authors contributed equally to this work.

§ Present address: Cubist Pharmaceuticals, 24 Emily Street, Cambridge, Massachusetts 02139.

|| Present address: Neurocrine Biosciences, 3050 Science Park Road, San Diego, California 92121.

⊥ Department of Chemistry, MIT.

▽ Department of Biology, MIT.

⊗ Abstract published in *Advance ACS Abstracts,* June 1, 1996.

[1] AdoHcy, *S*-adenosyl-L-homocysteine; ATP, adenosine 5′-triphosphate; AZT, 3′-azido-3′-deoxythymidine 5′-triphosphate; CDP, cytidine 5′-diphosphate; ClUDP, 2′-chloro-2′-deoxycytidine 5′-diphosphate; dNTP, 2′-deoxynucleoside 5′-triphosphate; DTT, dithiothreitol; EDTA, ethylenediamine tetraacetic acid; (*E*)-FMC, (*E*)-2′-(fluoromethylene)-2′-deoxycytidine; (*E*)- or (*Z*)-FMCDP, (*E*)- or (*Z*)-2′-(fluoromethylene)-2′-deoxycytidine 5′-diphosphate; Gn·HCl, guanidine hydrochloride; Hepes, *N*-(2-hydroxethyl)piperazine-*N*′-(2-ethanesulfonic acid); met-R2, R2 with its tyrosyl radical reduced; MS-CI, mass spectrometry by chemical ionization; NADPH, reduced β-nicotinamide adenine dinucleotide phosphate; N_3UDP, 2′-azido-2′-deoxyuridine 5′-diphosphate; PP_i, inorganic pyrophosphate; RDPR, ribonucleoside 5′-diphosphate reductase; RNR, ribonucleotide reductases; SA, specific activity; TFA, trifluoroacetic acid; TPCK, tosylphenylalanine chloromethyl ketone; TR, thioredoxin; Tris, tri(hydroxymethyl)aminomethane; TRR, thioredoxin reductase; TTP, thymidine 5′-triphosphate; Y•, tyrosyl radical on residue 122 of the R2 subunit; ZDDFA, (*Z*)-4′,5′-didehydro-5′-deoxy-5′-fluoroadenosine.

S0006-2960(96)00190-0 CCC: $12.00

terminators into DNA. This synergism has previously been exploited in the design of combination chemotherapy for treatment of HSV and HIV infections (Spector et al., 1985; Karlsson & Harmenberg, 1988; Ellis et al., 1989; Gao et al., 1993; Lori et al., 1994; Bianchi et al., 1994). The recent interest in (*E*)-FMC as a new antitumor agent has inspired us to investigate the detailed mechanism by which the corresponding diphosphate inhibits the *Escherichia coli* RNR. These studies have provided new insight into the catalytic capabilities of RNR and also provided evidence for nucleotide radical intermediates in this process.

E. coli ribonucleoside diphosphate reductase (RDPR) has been extensively investigated and serves as the prototype for the mammalian protein (Eriksson & Sjöberg, 1989; Stubbe, 1990a,b; Reichard, 1993). The enzyme consists of two subunits (R1, R2) which are each composed of two identical polypeptide chains. Each protomer of R1 (85.7 kDa) contains five cysteines required for catalysis (Mao et al., 1992a−c). In addition to the active site, R1 also contains sites for the binding of allosteric effectors (NTPs and dNTPs) that control both specificity and turnover. R2 contains a dinuclear iron center and tyrosyl radical cofactor essential for nucleotide reduction (Sjöberg et al., 1977).

A summary of the results with two well-characterized mechanism-based inhibitors, 2′-chloro-2′-deoxynucleotides (ClNDPs) and 2′-azido-2′-deoxynucleotides (N_3NDPs), is briefly presented to provide a background for understanding the experiments described in the present work. In 1976, Thelander and co-workers reported that both of these compounds inactivated *E. coli* RNR (Thelander et al., 1976). These preliminary studies suggested that the mechanisms of inactivation were unusual and that elucidation of their details would provide important insights about the mechanism of nucleotide reduction. Thus, over the past decade we (Stubbe & Kozarich, 1980b; Ator et al., 1984; Harris et al., 1984; Ator & Stubbe, 1985; Salowe et al., 1987; Ashley et al., 1988; Salowe et al., 1993) and others (Sjöberg et al., 1983) have unraveled these details, and from these studies a paradigm for inactivation by 2′-substituted 2′-deoxynucleotides has evolved (Scheme 1). In all cases inactivation is initiated by 3′-hydrogen atom abstraction by a Cys439 thiyl radical in R1, proposed to be generated by coupled electron and proton transfer to the tyrosyl radical on R2. Loss of X (as X^- or XH) from the nucleotide analog produces a radical intermediate which can be reduced from its top face (β-face) or its bottom face (α-face). Reduction from the β-face regenerates the thiyl radical, and hence the tyrosyl radical. Inactivation results in this case from nonspecific alkylation of R1 by 2-methylene-3(2*H*)-furanone (Scheme 1). This compound is generated in solution by spontaneous chemical decomposition of 3′-ketodNDP subsequent to its dissociation from the active site. We have previously described the observation that nucleophiles such as dithiothreitol (DTT) present during the inactivation studies can be used to prevent R1 alkylation and hence inactivation by this reactive furanone (Harris et al., 1984) (Scheme 1). Alternatively, if reduction occurs from the α-face, inactivation results from destruction of the essential tyrosyl radical on R2. The same 3′-ketodNDP is generated as well, and subsequent to its decomposition it also inactivates R1 by alkylation.

While ClNDP is the paradigm for the first type of inhibition and N_3NDP for the second, with most inhibitors we have investigated, inactivation results from contributions

Scheme 1

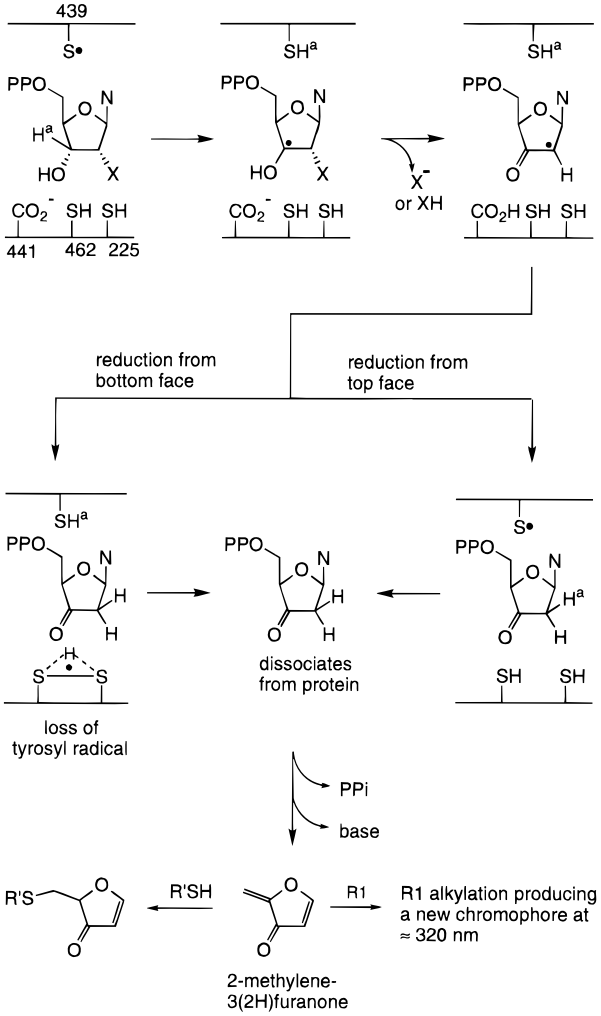

from both pathways (Harris et al., 1984; Baker et al., 1991). As described in detail subsequently, while the basic paradigm pertains to the inhibition of RDPR by FMCDP, subtle variations from other inhibitors previously studied make the mode of inactivation by this inhibitor unique.

MATERIALS AND METHODS

Materials. R1 [ϵ_{280nm} = 189 000 M^{-1} cm^{-1}; specific activity (SA), 1500−1700 nmol min^{-1} mg^{-1}], and R2 (ϵ_{280nm} = 130 500 M^{-1} cm^{-1}; SA 7700−8000 nmol min^{-1} mg^{-1}) were prepared as described by Salowe and Stubbe (1986). The R1 mutants C225S, C462S, C439S, and C754/759S were isolated from K38-overproducing strains as previously described (Mao et al., 1989, 1992a,c). The mutant E441QR1 was prepared using a Sculptor *in vitro* mutagenesis kit from Amersham. The primer for E441QR1 (5′ CCT GTG CCT GCA GAT AGC CCT GC 3′) was synthesized at Research Genetics and purified before use with a NAP5 column from Pharmacia Biotech. Pre-reduced R1 was prepared and characterized as previously described (Lin et al., 1987). *E. coli* thioredoxin (TR) was isolated from SK3981 (Lunn et al., 1984) with an SA of 36 units mg^{-1}, and thioredoxin reductase (TRR) was isolated from K91/pMR14 (Russel & Model, 1985) with an SA of 1000 units mg^{-1}. Calf intestine alkaline phosphatase was purchased from Boehringer Mannheim. Adenosine 5′-triphosphate (ATP), cytidine 5′-diphosphate (CDP), thymidine-5′-triphosphate (TTP), reduced

β-nicotinamide adenine dinucleotide phosphate (β-NADPH), and tosylphenylalanine chloromethyl ketone (TPCK)-treated trypsin were obtained from Sigma. Trifluoroacetic acid (TFA) was obtained from Aldrich. Urea (molecular biology grade, American Bioanalytical) was purified using a mixed-bed Dowex-AG-501-X8 (D) resin (Bio-Rad). [U-^{14}C]CDP was purchased from New England Nuclear (SA, 532 mCi mmol^{-1}) or Moravek (SA, 400 mCi mmol^{-1}) and mixed with unlabeled CDP prior to use. DTT was purchased from Mallinckrodt.

Methods. UV−vis spectroscopy was carried out using an HP8452A diode array spectrophotometer. Electron spin resonance (EPR) spectra at 9 GHz were acquired on a Bruker ESP-300 spectrometer at 100 K. Spin quantitation was achieved with a 1.0 mM $CuSO_4$, 2 M $NaClO_4$, 0.01 M HCl, 20% (v/v) glycerol standard ($g = 2.18$) (Malmström et al., 1970). Fluoride analyses were made with an Orion 96-09 fluoride combination electrode using methods previously described (Stubbe & Kozarich, 1980a). Liquid scintillation counting was performed on a Packard 1500 analyzer with Scint-A XF (Packard) scintillation fluid. HPLC for peptide mapping was performed on a Beckman System Gold with a Vydac C-18 RP-column (4 mm × 25 cm). Solvent system I consisted of solvent A (0.1% aqueous TFA) and solvent B (80% aqueous acetonitrile, 0.07% TFA). Solvent system II consisted of solvent C (5 mM potassium phosphate, pH 6.2) and solvent D (20% solvent C, 80% acetonitrile).

*(E)-2′-(Fluoromethylene)-2′-deoxycytidine-5′-monophosphoric Acid [(E)-FMCMP] (**1**).* Compound **1** was prepared by a modification of the procedure of Yoshikawa et al. (1967). To 253 mg (1.0 mmol) of (*E*)-FMC (McCarthy et al., 1991; Matthews et al., 1993) in 2.0 mL of triethylphosphate under N_2, cooled in an ice bath, was added 0.15 mL (1.6 mmol) of $POCl_3$ dropwise by syringe. After 40 min, the ice bath was removed. The reaction mixture was stirred for 3 h, poured into an equal volume of water, and stirred for 5 min. Aqueous 1 M NaOH was added (waiting for the pH to adjust after each few drops) until the pH of the solution had reached 3. Water was added and the mixture was extracted three times with 20 mL of diethyl ether. The aqueous layer was passed through a charcoal column (7 g, Aldrich Nucleotide desalting grade). The column was eluted with water followed by 0.25 M NH_4HCO_3 in 1:1 ethanol−water. Fractions were collected and monitored by HPLC (described below). The fractions containing nucleotides were combined, and solvents were removed in vacuo, affording a white powder. HPLC analysis (Deltapak C-18, 100 Å, 3.9 mm × 30 cm; eluted with 7% MeOH and 93% 0.01 M NH_4HCO_2, pH 6; flow rate, 2.0 mL/min) of this material showed a mixture of two products consisting of **1** (55% yield, retention time 1.32 min) and the 3′,5′-cyclic monophosphate of FMC identified by FAB anion mass spectroscopy (32% yield, retention time, 5.94 min). The mixture was purified on a Deltapak C18-100 Å preparatory column (19 mm × 30 cm) equilibrated in 7% MeOH and 93% 0.01 M NH_4HCO_2, pH 6 (flow rate of 9 mL/min). The methanol content was then increased to 15% in increments, fractions containing **1** were pooled, and the solvent was removed in vacuo (157 mg, 54%). FAB-MS (negative ion) 336 (M − H).

*(E)-FMCDP (**2**).* The ammonium salt of **1** (15.5 mg, 0.043 mmol) was converted to the diphosphate by the procedure of Hoard and Ott (1965). The reaction was allowed to proceed for 28 h. Subsequent to workup, the crude mixture was lyophilized and the residue was dissolved in 1−2 mL of water and allowed to stand for 1 h. Compound **2** was purified on a Hamilton PRP-X100 column (75 mm × 21.5 mm) eluting with 0.1 M NH_4HCO_3 in 12% CH_3CN/88% H_2O (buffer A) for 20 min at a flow rate of 12 mL/min followed by elution with a 1:1 mixture of buffer A and buffer B (20% CH_3CN/80% 0.6 M NH_4HCO_3 in H_2O). The appropriate fractions were combined and repeatedly lyophilized from water to afford 6.2 mg (32%) of the diphosphate. FAB-MS (negative ion) 416 (M − 1). ^{19}F NMR (D_2O) δ ppm −125.20 (d, $J_{FH} = 78.2$ Hz); ^{1}H NMR (D_2O) δ ppm 7.83 (d, 1H, $J = 7.8$ Hz), 6.86 (m, 1H, $J = 76$ Hz, vinyl-H), 6.89 (m, 1H, 1′-H), 6.16 (d, 1H, $J = 7.8$ Hz), 5.28 (m, 1H, 3′-H), 4.21 (m, 3H, 4′-H and 5′-H); UV−vis (H_2O) $\epsilon_{270nm} = 8520$ M^{-1} cm^{-1}.

Synthesis of [5-^{3}H]-(E)-FMC. 5-Iodo-(*E*)-FMC-3′,5′-diacetate (0.5 mmol) was prepared from (*E*)-FMC by treatment with acetyl chloride (3.2 equiv) in acetic acid to provide the 3′,5′-diacetate hydrochloride salt as a white crystalline solid in 43% yield, MS-CI 342 (M + H). The diacetate was treated with silver trifluoroacetate (2.4 equiv) and iodine (3.6 equiv) in dioxane−ethanol at 0 °C to provide the 5-iodo derivative as an oil in 90% yield; MS-CI 468 (M + H); ^{19}F NMR ($CDCl_3$) δ ppm −120.76 (d, $J_{FH} = 72$ Hz); ^{1}H NMR ($CDCl_3$) δ ppm 7.87 (s, 1H, 6-H), 6.95 (dt, 1H, $J = 72.5$ Hz, 6′-H), 6.83 (m, 1H, 1′-H), 5.98 (m, 1H, 3′-H), 4.3−4.5 (m, 1H, 4′-H), 3.65−3.80 (m, 2H, 5′-H), 2.20 (s, 3H, OAc), 2.13 (s, 3H, OAc).

The above iododiacetate was sent to New England Nuclear for tritium incorporation by reductive deiodination. The reduction was carried out with $^3H_2$, NaOAc, and 5% Pd/C in ethanol, yielding 25 mCi of crude diacetate. The product was purified on silica gel preparative TLC plates with 20% MeOH/CH_2Cl_2. The diacetate (5.1 mCi) was treated with 1 mg of K_2CO_3 in 500 μL of ethanol to give 4.6 mCi of [5-^{3}H]-(*E*)-FMC (SA, 8.6 mCi/μmol).

Synthesis of [5-^{3}H]-(E)-FMCDP. A 774 μCi sample of the [^{3}H]-(*E*)-FMC was treated with 15 μL of a $POCl_3$/triethylphosphate (0.3:1.4 v/v) solution to give the monophosphate. The [^{3}H]monophosphate was identified by comparison with unlabeled (*E*)-FMCMP and was purified on a Hamilton 10 μm PRP-X100 column (250 mm × 4.1 mm) using a gradient of ammonium bicarbonate and acetonitrile. Lyophilization of the appropriate fractions provided the monophosphate. The [5-^{3}H]-(*E*)-FMCMP (250 μCi, 30 nmol) was then incubated for 1 h at room temperature in 12 mM Hepes, pH 7.6, with 0.25 units of bovine nucleoside monophosphate kinase, 1 mM ATP, 0.07 mM KCl, and 0.2 mM $MgSO_4$. Aliquots of the incubation mixture were purified on a Hamilton 10 μm PRP-X100 column (250 mm × 4.1 mm) and eluted with a gradient of ammonium bicarbonate and acetonitrile. The product was detected at A_{254nm}, and the fractions were lyophilized to dryness, dissolved in 50% ethanol, and stored at −20 °C. Purity was checked by HPLC using a Flo-One Radioactive Flow detector (Radiomatic Instruments), indicating an SA of 8.6 mCi/μmol.

Synthesis of [6′-^{14}C]-(E)-FMC. [6′-^{14}C]-(*E*)-FMC was prepared by the procedure of Matthews et al. (1993) starting with the treatment of a mixture of methyl[^{14}C]phenyl sulfoxide (320 mCi, 59.3 mCi/mmol, 5.40 mmol) and unlabeled methylphenyl sulfoxide (7.35 mmol) with (diethylamino)sulfur trifluoride. In the last step of the reaction

sequence the [6′-^{14}C]-(*E*)-FMC was crystallized from MeOH (10 mL) and EtOAc (40 mL) by storage at −20 °C overnight. Yield: 601 mg (2.34 mmol, 57.8 mCi). MS-FAB 258 (M + 1), 260 (M + 3). The product was judged to be homogeneous by HPLC (Zorbax RxC8, 250 mm × 4.6 mm column).

Synthesis of [6′-^{14}C]-(E)-FMCDP. [6′-^{14}C]-(*E*)-FMC (3.5 μCi, 350 nmol) was converted to [6′-^{14}C]-(*E*)-FMCDP as described above for the preparation of [5-^{3}H]-(*E*)-FMCDP. Purity was checked by HPLC (SA, 10 μCi/μmol).

Synthesis of (Z)-FMCDP. (*Z*)-FMCMP was prepared from the (*Z*)-nucleoside (Matthews et al., 1993) as described above. After charcoal treatment, no HPLC purification was necessary since the cyclic phosphate was not formed. The monophosphate was subsequently converted into the ammonium salt of the diphosphate as described above. ^{19}F NMR (D_2O) δ −124.87 (d, J_{FH} = 78.9 Hz); FAB-MS negative ion (M − 1) 416; UV−vis (H_2O) ϵ_{268nm} = 6830 M^{-1} cm^{-1}.

Time Dependent Inactivation of RDPR by FMCDP. The reaction mixtures contained in a final volume of 650 μL: Hepes assay buffer (50 mM Hepes, 15 mM $MgSO_4$, 1 mM EDTA, pH 7.6), 15 μM R1, 15 μM R2, either 1.6 mM ATP or 0.2 mM TTP, and various concentrations (0−300 μM) of (*Z*)- or (*E*)-FMCDP. All of the reactions were performed aerobically at 25.0 (±1.0) °C. In addition, reactions contained 10 mM DTT as reductant, 4.5 μM TR, 0.2 μM TRR, and 0.5 mM NADPH as reductant, or no reductant and pre-reduced R1. The reaction was initiated by the addition of FMCDP, and at various time points, 10 μL of the mixture was removed and diluted into 90 μL of an assay mixture containing in final concentrations: 1.0 mM [U-^{14}C]-CDP (SA, 5.3 × 10^5 cpm/μmol), ATP (1.6 mM), NADPH (1.0 mM), TR (4.5 μM), TRR (0.2 μM), and Hepes assay buffer. Each reaction was incubated for 5 min at 25 °C and stopped by immersing the reaction vessel in a boiling water bath for 3 min. Upon cooling the reaction was made 0.16 M in Tris·HCl (pH 8.0), treated with 2 units of *E. coli* alkaline phosphatase, and incubated at 37 °C for 1 h. Carrier deoxycytidine (dC, 80 nmol) was added, and the dC was quantitated by the method of Steeper and Steuart (1970).

Time Dependent Loss of Tyrosyl Radical and R1 Activity. The inactivation reaction was carried out in a cuvette at 25 °C under aerobic conditions as described above. Time dependent loss of the tyrosyl radical was monitored by change in A_{412nm} using the previously reported drop-line correction at 412 nm, $[A_{412nm} - (2A_{406nm} + 3A_{416nm})/5]$, with ϵ = 1920 M^{-1} cm^{-1} (Bollinger et al., 1991). Simultaneously, inactivation of R1 was monitored by removing 8 μL aliquots at various time points which were added to 352 μL of an assay solution containing: 10 μM R2 (30-fold excess of R2 over R1), 1.0 mM [U-^{14}C]CDP (SA, 1.8 × 10^5 cpm/μmol), 1.6 mM ATP, 10 mM DTT, and Hepes assay buffer. The reactions were quenched after 10 min with 100 μL of 5% $HClO_4$ and neutralized with 90 μL of 1 M aqueous KOH. Deoxycytidine was quantitated as described above.

EPR Studies on the Interaction of (Z)- and (E)-FMCDP with RDPR. A spectrum was recorded of the tyrosyl radical before addition of the inhibitor as described in the legend of Figure 3. This sample contained in a final volume of 250 μL: 75 μM R1, 75 μM R2, 1.6 mM ATP, and 50 mM Hepes assay buffer (pH 7.6). The reaction was initiated by addition of (*E*)-FMCDP to a final concentration of 300 μM. The reaction mixture was incubated at 25 °C for 1 min and frozen in liquid nitrogen. An EPR spectrum was then recorded (Figure 3).

Identification of Products Accompanying Inactivation of RDPR. RDPR (15 μM) was incubated, typically 30 min at 25 °C, with FMCDP under the conditions described above in a final volume of 1.8 mL. The small molecular weight components were separated from the proteins by Centricon-30, and the protein solution was washed once with 1 mL of 50 mM Hepes assay buffer, pH 7.6. The combined filtrates were lyophilized, and the residue was dissolved in 1 mL of water. The fluoride content was determined as previously described (Stubbe & Kozarich, 1980a).

Subsequent to analysis for fluoride, 250 μL of 0.5 M Tris buffer, pH 8.4, and 5 units of calf intestine alkaline phosphatase were added to the mixture and incubated for 2 h at 37 °C. The mixture was then passed through a 0.5 cm × 10 cm Dowex anion exchange column in the tetraborate form (Steeper & Steuart, 1970). The column was eluted with 10 mL of water, the resulting solution was lyophilized, and the residue was redissolved in 500 μL of water. The sample was then chromatographed on an Econosil C-18 Alltech RP column at a flow rate of 1.0 mL min^{-1} using isocratic elution with 5 mM potassium phosphate buffer, pH 6.8, for 10 min, followed by a linear gradient to 30% methanol/70% phosphate buffer over 30 min. Retention times: cytosine, 5 min; *E*-FMC, 14 min; *Z*-FMC, 18 min. Cytosine was identified and quantitated by its characteristic shift in λ_{max} from 267 nm (ϵ = 6600 M^{-1} cm^{-1}) to 276 nm (ϵ = 9100 M^{-1} cm^{-1}) when the pH was changed from 6.8 to 1.6, respectively.

The stabilities of (*E*)- and (*Z*)-FMCDPs (60 nmol) were studied under identical conditions as described above. A recovery of 62% was obtained with (*Z*)-FMCDP and 83% for (*E*)-FMCDP. No cytosine release was observed.

Radiolabeling of RDPR with [5-^{3}H]-(E)-FMCDP. A typical reaction contained the following in a final volume of 650 μL: Hepes assay buffer, 15 μM pre-reduced R1, 15 μM R2, 1.6 mM ATP, and 38 μM (*E*)-FMCDP (SA, 1.34 × 10^6 cpm/μmol). A control was run in which met-R2 (R2 in which the tyrosyl radical has been reduced) replaced R2. Reaction and control were incubated for ∼120 s. 200 μL of each was then loaded on a G-25 Sephadex column (20 mL) equilibrated and eluted with 2 M guanidine hydrochloride (Gn·HCl) in 5 mM Hepes (pH 7.7). The protein fractions were combined and a difference spectrum was taken after adjusting A_{280nm} to be identical in the reaction and the control. The protein was quantitated and analyzed for radiolabel by liquid scintillation counting.

A second aliquot (200 μL) of the reaction and of the control was loaded on a G-25 column (20 mL) equilibrated and eluted with 50 mM Hepes buffer. A difference spectrum was again taken. The protein was quantitated and analyzed for radioactivity. This solution of labeled protein was then incubated for 24 h at 37 °C, passed through a second G-25 Sephadex column (20 mL total volume), and again analyzed for radioactivity.

Radiolabeling of RDPR with [6′-^{14}C]-(E)-FMCDP. The inactivation mixture contained the following in a final volume of 5 mL: 50 mM Hepes assay buffer, 1.6 mM ATP, 15 μM R1, 45 μM R2, 3 mM DTT, and 60 μM [6′-^{14}C]-(*E*)-FMCDP (SA, 1.6 × 10^6 cpm μmol^{-1}), and the mixture was incubated for 15 min at 25 °C. At the end of this period the protein was assayed for activity. The small molecules were removed

by centrifugation in a Centricon-30. The protein solution was then loaded onto a dATP Sepharose affinity column (2.5 cm × 20 cm) (Berglund & Eckstein, 1974) equilibrated with 50 mM Tris, pH 7.6. The flow through was analyzed by A_{280nm} and the R2-containing fractions were analyzed by liquid scintillation counting. The column was washed with an additional 100 mL of buffer prior to changing the eluent to 50 mM Tris·HCl, 10 mM ATP, pH 7.6. The first 50 mL of flow through containing ATP was pooled and concentrated by ultrafiltration using an Amicon-YM 30 membrane. The concentrated protein solution was then diluted with 50 mM Tris, pH 7.6, and reconcentrated to remove ATP. This procedure was repeated several times. The resulting R1 solution was analyzed by liquid scintillation counting.

UV−Vis Spectroscopic Analysis of Inactivated RDPR. Reactions were performed in 400 μL of Hepes assay buffer containing 15 μM R1, 15 μM R2, 1.6 mM ATP, and 60 μM (*E*)-FMCDP or 150 μM (*Z*)-FMCDP. The control reactions were identical except that R2 was replaced by met-R2. The time dependent change in absorbance at 334 nm was recorded, after 20 min both reactions and controls were loaded on Sephadex G-50 columns (1.0 cm × 25 cm), and the proteins were eluted with 50 mM Tris buffer, pH 7.6. After reconcentration of the protein-containing fractions, difference spectra were recorded on a Cary-210 after equalizing the protein concentrations (A_{280nm}) in the inactivated protein and control solutions. The proteins were then denatured by the addition of Gn·HCl to a final concentration of 6 M. The samples were loaded on Sephadex G-50 columns (1.0 cm × 25 cm) equilibrated and eluted with 50 mM Tris, 2 M Gn·HCl. After reconcentration of the protein, another difference spectrum was taken.

RESULTS

Time Dependent Inactivation of RDPR with (Z)-FMCDP and (E)-FMCDP. Incubation of pre-reduced RDPR with varying concentrations of inhibitor in the presence of ATP as an allosteric effector showed that a ~2-fold excess of (*E*)- or (*Z*)-FMCDP resulted in complete enzyme inactivation in a time dependent fashion with a $t_{1/2}$ of less than 20 s, as indicated for the *E*-isomer in Figure 1. The rates of inactivation in the presence of the reducing system, TR/TRR/NADPH or DTT, were slower than when pre-reduced RDPR was used (data not shown). The kinetics of inactivation with both inhibitors and under a variety of conditions were multiphasic due to multiple modes of inhibition and thus have prevented determination of accurate kinetic parameters.

Inactivation of both R1 and R2 Result from Incubation of RDPR with (Z)-FMCDP or (E)-FMCDP. Previous studies of RDPR inactivation by mechanism-based inhibitors have established that inhibition can be attributed to several distinct processes including loss of the tyrosyl radical cofactor (Y•) on R2 or covalent modification of R1. The multiphasic kinetics and the requirement of multiple turnovers for inactivation of RDPR by FMCDP suggested that the activities of both R1 and R2 be examined. Since loss of Y• on R2 is synonymous with R2 inactivation, its A_{412nm} was monitored during the course of the reaction. Time and concentration dependent reduction of Y• was observed with both isomers and is shown in Figure 2 for (*E*)-FMCDP. Furthermore, the rate of Y• loss was slower than the rate of RDPR inactivation

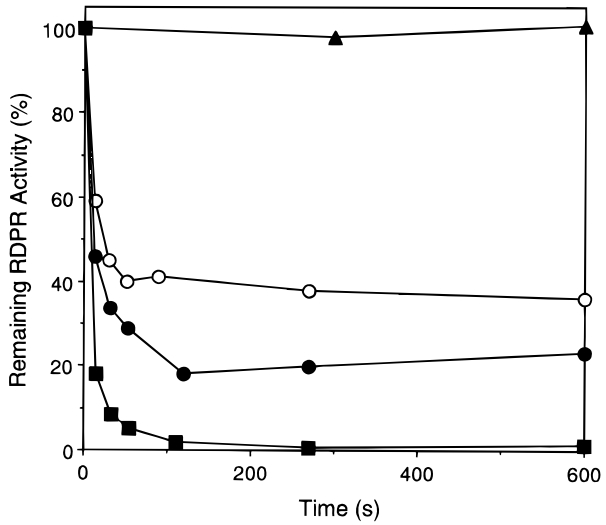

FIGURE 1: Concentration and time dependent inactivation of RDPR by (*E*)-FMCDP in the absence of reducing equivalents. Conditions: [pre-reduced R1], [R2] = 15 μM and [ATP] = 1.6 mM, 25 °C; (▲) 0 μM (*E*)-FMCDP, (○) 7.5 μM (*E*)-FMCDP, (●) 15 μM (*E*)-FMCDP, and (■) 30 μM (*E*)-FMCDP.

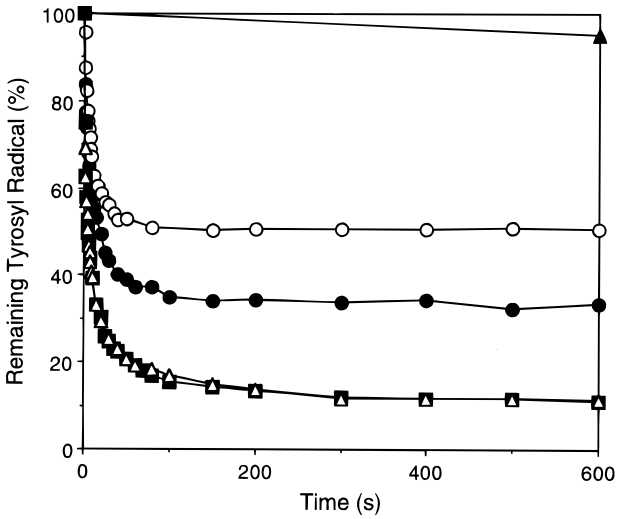

FIGURE 2: Concentration and time dependent tyrosyl radical loss on R2 with (*E*)-FMCDP in the absence of reducing system. Conditions: [pre-reduced R1], [R2] = 15 μM and [ATP] = 1.6 mM, 25 °C; (▲) 0 μM (*E*)-FMCDP, (○) 7.5 μM (*E*)-FMCDP, (●) 15 μM (*E*)-FMCDP, (■) 30 μM (*E*)-FMCDP, and (△) 60 μM (*E*)-FMCDP. Note: R2 is prone to proteolytic degradation at its C-terminus, which renders it inactive due to its inability to bind R1. The R2 preparation used in this experiment contained about 10% of proteolyzed enzyme accounting for the residual radical content at t = 10 min observed in the experiments with 30 or 60 μM (*E*)-FMCDP. Experiments conducted with more homogeneous R2 preparations show complete loss of the tyrosyl radical.

(data not shown), suggesting an R1 component to the inhibition. The effect of the inhibitors on the activity of R1 was therefore also examined. At certain time points after initiation, aliquots of the reaction mixture were diluted into an assay solution containing a 30-fold excess of R2. Within the first time point (30 s), 90% loss of R1 activity was observed with both inhibitors. These results indicate that inactivation of R1 and R2 is required to account for inactivation of RDPR.

EPR Studies on the Interaction of (Z)- and (E)-FMCDP with RDPR. Studies on the interaction of N_3UDP with RDPR have shown that rapid loss of Y• on R2, responsible

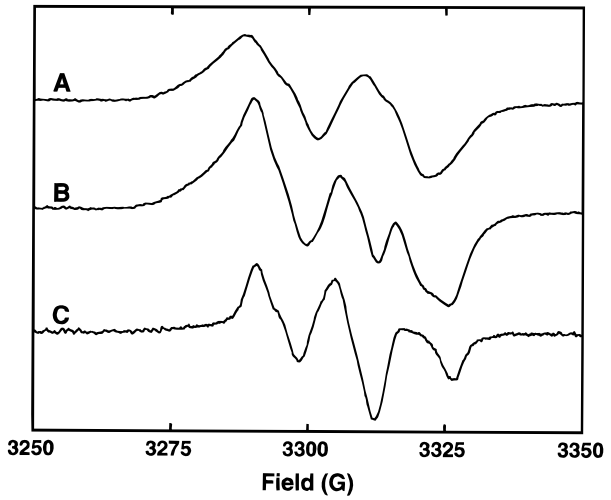

FIGURE 3: A. EPR spectrum of the tyrosyl radical present in a frozen solution containing 75 μM RDPR and 1.6 mM ATP. B. EPR spectrum taken 1 min after incubation of the sample with 300 μM (*E*)-FMCDP. C. New EPR signal obtained by subtraction of a fractional amount (70%) of the tyrosyl radical signal. All EPR spectra were acquired under the following conditions: microwave frequency, 9.43 GHz; temperature, 100 K; microwave power 100 μW; modulation amplitude 4 G; modulation frequency 100 kHz; time constant, 0.126 s.

for enzyme inactivation, is accompanied by the generation of a new, inhibitor-derived radical that is covalently attached to a cysteine of R1 (van der Donk et al., 1995). Therefore, the observation of rapid loss of Y$^\bullet$ during the inactivation of RDPR by FMCDP prompted us to investigate whether a new protein- or nucleotide-based radical could be detected by EPR spectroscopy. As shown in Figure 3 for (*Z*)-FMCDP a new signal is observed (Figure 3B) that is different from that of Y$^\bullet$ of R2 (Figure 3A). A closer examination of the spectrum in Figure 3B suggests that it is composed of two species, one being residual Y$^\bullet$. To obtain a spectrum of the new radical species, increasing amounts of the Y$^\bullet$ signal were subtracted from the spectrum in Figure 3B, ultimately giving rise to the signal shown in Figure 3C. The structure responsible for this signal is at present unknown, but preliminary EPR studies using isotopically labeled FMCDP suggest that it is nucleotide derived. Evidence in support of this proposal comes from power saturation analysis of this signal. Given that Y$^\bullet$ is adjacent to the iron cluster and that the new signal is likely associated with a nucleotide-derived radical on R1, 35 Å removed from the iron cluster (Uhlin & Eklund, 1994), the signals for Y$^\bullet$ and the new species should show very distinctive microwave power behavior. As expected, a value of $P_{1/2} = 50$ mW was observed for the Y$^\bullet$ signal at 100 K, which was at least 2 orders of magnitude higher than that of the second component.[2] This signal was observed with both (*E*)- and (*Z*)-FMCDP, irrespective of the presence or absence of external reducing equivalents (DTT or TR/TRR/NADPH).

Identification of Products Accompanying RDPR Inactivation. Previous studies with 2′-deoxy-2′-halonucleotides revealed that inactivation of RDPR was accompanied by nucleic acid base and halide release (Scheme 1). To characterize the products formed with (*Z*)- and (*E*)-FMCDP, the protein was separated from small molecular weight compounds by means of centrifugation through a membrane with a 30 kDa cutoff. The resulting solutions were analyzed for fluoride ion and cytosine release and compared to control samples in which R2 had been replaced with met-R2. The results indicate that for each isomer similar quantities of fluoride and cytosine were produced per RDPR inactivated (Table 1).

Table 1: Fluoride and Cytosine Release Data for the Incubation of 15 μM RDPR (R1:R2 1:1) with 60 μM of (*E*)-FMCDP or (*Z*)-FMCDP in the Presence of DTT

entry no.	R1 or R1 analog	inhibitor	cytosine released per R1	fluoride released per R1
1	wt-R1	(*E*)-FMCDP	0.5 ± 0.1	1.4 ± 0.1
2	wt-R1	(*Z*)-FMCDP	0.5 ± 0.1	1.2 ± 0.1
3	C225S	(*Z*)-FMCDP	1.1 ± 0.05	1.4 ± 0.1
4	C462S	(*Z*)-FMCDP	0.7 ± 0.15	0.6 ± 0.15
5	C439S	(*Z*)-FMCDP	*a*	*a*
6	E441Q	(*E*)-FMCDP	1.4 ± 0.02	*b*

[a] Quantities are at or below our experimental limits of detection (see Materials and Methods). [b] Not determined.

Table 2: Alkylation of R1 after Incubation of 15 μM RDPR (R1:R2 1:1) with 60 μM of [^{14}C]-(*E*)-FMCDP in the Presence of DTT

entry no.	R1 or R1 analog	time (h)[a]	remaining Y$^\bullet$ (%)[b]	equiv of radiolabel per equiv of R1
1	wt-R1	0.3	0	0.92 ± 0.1
2	C225S	0.5	0	0.70 ± 0.05
3	C462S	3	40	0.75 ± 0.05
4	C439S	3	100[c]	*c*
5	E441Q	3.5	0	0.24 ± 0.02
6	C754/759S	0.5	0	0.70 ± 0.05

[a] The extent of radiolabeling was determined after incubation for the indicated time periods. For all proteins except C462S and C439S the inactivation was complete as monitored by the loss of the tyrosyl radical (see also Figure 5). [b] The tyrosyl radical content after incubation for the indicated time periods. [c] No label or tyrosyl radical loss detected in comparison with control samples.

Radiolabeling of RDPR with [5-^{3}H]-(E)-FMCDP. The measurement of 1.2−1.4 equiv of fluoride and 0.5 equiv of cytosine per inactivation event (Table 1) indicated that ∼1 equiv of a nucleotide was missing. Therefore, [5-^{3}H]-(*E*)-FMCDP was prepared to more accurately determine its fate. Incubation of RDPR with [5-^{3}H]-(*E*)-FMCDP in the absence of DTT followed by removal of small molecules via centrifugation followed by Sephadex G-50 column chromatography revealed 1.0 equiv of ^{3}H per RDPR in addition to the 0.5 equiv of cytosine. Although the label was stable during gel filtration at 4 °C, all radioactivity was liberated from the protein as cytosine upon standing at 37 °C for 24 h. Moreover, rechromatography of [^{3}H]RDPR in 2 M Gn·HCl led to release of all radiolabel as cytosine.

Radiolabeling of RDPR with [6′-^{14}C]-(E)-FMCDP. The fate of the sugar moiety of FMCDP subsequent to inactivation was investigated by synthesis of [6′-^{14}C]-(*E*)-FMCDP. Incubation of RDPR with [6′-^{14}C]-(*E*)-FMCDP in the presence of DTT, followed by separation of R1 and R2 using a dATP affinity column (Berglund & Eckstein, 1974), revealed 0.9 equiv of radiolabel/R1 (Table 2). No radioactivity was associated with R2. Denaturation of R1 in 6 M Gn·HCl, followed by gel filtration chromatography in 2 M Gn·HCl

[2] In order to determine the microwave power dependence of the amplitude of the new radical EPR signal, the signal of Y$^\bullet$ was subtracted from spectra obtained at various powers. However, the low signal-to-noise ratio of the difference spectra obtained at low microwave powers precluded an exact measurement of $P_{1/2}$ for the new radical.

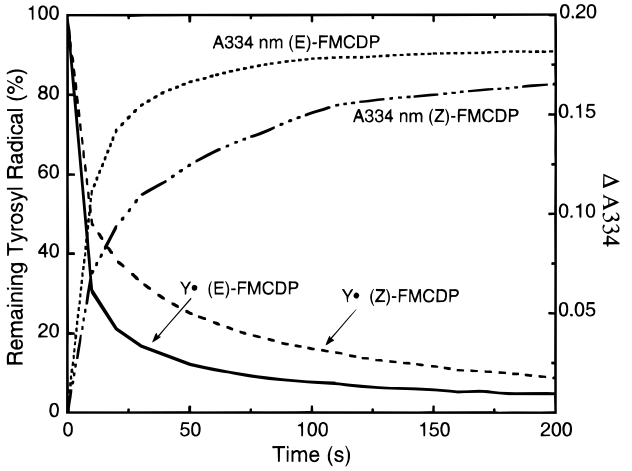

FIGURE 4: Correlation between the time dependent change in absorbance at 334 nm and tyrosyl radical reduction in the reaction of 15 μM pre-reduced R1 with 60 μM (*Z*)-FMCDP or (*E*)-FMCDP. (—•••—) A_{334nm} (*Z*)-FMCDP; (— — —) Y• loss (*Z*)-FMCDP; (- - -) A_{334nm} (*E*)-FMCDP; (—) Y• loss (*E*)-FMCDP. In both reactions [R2] = 15 μM, [ATP] = 1.6 mM. The reduction of the tyrosyl radical was complete after 10 min for both reactions, and in both cases ΔA_{334nm} was 0.18 at the end point of the reaction.

established that the label remained covalently attached to R1. Thus, efforts were initiated to purify a radiolabeled peptide via HPLC chromatography, subsequent to cleavage of R1 by trypsin digestion. However, incubation of R1 with 30 mM DTT in 2 M Gn·HCl, conditions used to prepare the protein for alkylation of its cysteines, resulted in liberation of 60% of the label from R1. Therefore, radiolabeled R1 was digested without prior cysteine alkylation, and the peptides were purified by HPLC chromatography on a Vydac column at pH 2 or pH 6.0. Under both conditions analysis of fractions for radioactivity revealed scrambling of the label. In an effort to stabilize the radiolabeled adduct, R1 inactivated with (*E*)-FMCDP was treated with NaB^3H_4 under native and denaturing conditions.[3] In neither case could a specific peptide be isolated that had been modified by FMCDP.

Influence of DTT on Radiolabeling and Chromophore Formation. Previous studies of mechanism-based inhibitors of RDPR have established that inactivation is often accompanied by protein alkylation by 2-methylene-3(2*H*)-furanone (Scheme 1), which eventually results in the appearance of a new protein-associated chromophore at ~320 nm. In many cases DTT has been shown to protect the protein from covalent labeling and chromophore development by trapping of the furanone (Harris et al., 1984). As indicated in Figure 4, when (*Z*)- or (*E*)-FMCDP was incubated with RDPR in the absence of DTT, rapid formation of a new chromophore with λ_{max} at 334 nm was detected. Under these conditions [6′-^{14}C]-(*E*)-FMCDP produced 1.2 equiv of radiolabel bound to R1. It was anticipated that if DTT trapped a reactive sugar moiety, it would reduce the amount of radiolabel and the amount of chromophore on R1. As indicated above, in the presence of DTT only 0.90 equiv of label was bound to R1 and no chromophore was detected. In both the presence and absence of DTT rapid loss of Y• was observed. These results are consistent with trapping of a furanone-like species by DTT and in combination with the results using [5-^{3}H]-(*E*)-FMCDP, suggest ~30% of the labeling events are associated with a furanone-type pathway. As will be discussed subsequently, however, other interpretations of these results are also possible.

Interaction of (E)-FMCDP with R1 Mutants C225S, C462S, C439S, and C754/759S: Radiolabeling of R1. Studies of the phenotypes of a number of site-directed mutants of the R1 subunit have contributed greatly to our current understanding of the mechanism of substrate reduction catalyzed by RDPR (Åberg et al., 1989; Mao et al., 1989,1992a−c). The results of these studies in combination with the recently published crystal structure of the R1 from *E. coli* (Uhlin & Eklund, 1994) strongly implicate the presence of cysteines 225, 439, and 462 in the active site of the enzyme, while cysteines 754 and 749 are located on a flexible tail and shuttle reducing equivalents into the active site. The studies described above failed to identify a peptide alkylated by [6′-^{14}]-(*E*)-FMCDP. Therefore, in an alternative effort to obtain information on the site of radiolabeling by (*E*)-FMCDP, its interaction with cysteine mutants of R1 was examined. DTT was used in the reaction mixture to prevent possible covalent modification by a furanone equivalent from solution. The results of these studies are shown in Table 2 and indicate that none of these cysteines, with the possible exception of C439, is responsible for alkylation. Since the inactivation is thought to be initiated by the C439 thiyl radical, it is not surprising that no covalent modification of C439SR1 was detected. Thus, the possibility that C439 is the site of alkylation cannot be experimentally examined using site-directed mutants. For the other three cysteine mutants the radiolabel remained bound even after denaturation in Gn·HCl, and as in the case of wt-R1, addition of 30 mM DTT led to its release.

Interaction of FMCDP with R1 Mutants C225S, C462S, C439S, and C754/759S: Y• Loss, Fluoride and Cytosine Release, and Chromophore Formation. In order to complete the characterization of the interaction of FMCDP with the cysteine mutants, Y• loss on R2 was examined and the products of inactivation were analyzed. As shown in Figure 5 loss of Y• was rapid and complete with C225SR1 and C754/759SR1. The extent of loss of the radical was substantially reduced for C462SR1 (~30% radical loss after 10 min and ~63% loss after 3 h). As expected given its central role in catalysis, C439SR1 did not show any tyrosyl radical loss in comparison with control samples.

The results of cytosine and fluoride release are summarized in Table 1. As expected for C439SR1, neither fluoride nor cytosine release was detected. The C462SR1 produced 0.6 equiv of F^-/R1 and 0.7 equiv of cytosine, while C225SR1 gave 1.4 equiv of fluoride and 1.1 equiv of cytosine. Thus, in the case of each cysteine mutant, the fluoride release is not equivalent to the sum of cytosine released and R1 alkylated as seen for wt-R1 (Tables 1 and 2).

Finally, the effect of the mutant proteins on chromophore formation was examined in the absence of DTT. Incubation of C225SR1 and C754/759SR1 with (*E*)-FMCDP resulted in rapid production of a new absorbance feature with a λ_{max} at 334 nm (data not shown). The intensity of this new absorbance and the rate of its formation were comparable to that observed with wt-R1 under identical conditions. Studies with C462SR1 also indicated the formation of the new chromophore at 334 nm, but at a much slower rate, while no chromophore was detected for C439SR1.

[3] Experimental details of these studies can be found in the supporting information.

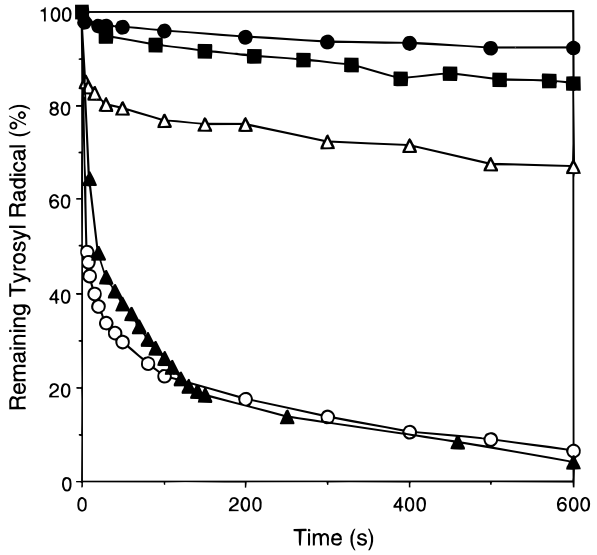

FIGURE 5: Tyrosyl radical reduction with mutant R1s in the absence of external reductants. For all experiments [pre-reduced R1 or R1 analogs] = [R2] = 15 μM, [ATP] = 1.6 mM. (●) C439S, [(*Z*)-FMCDP] = 300 μM. The small decrease in tyrosyl radical content over 10 min is similar to that seen in control samples without added inhibitor; (△) C462S, [(*Z*)-FMCDP] = 60 μM; (▲) C754/759S, [(*E*)-FMCDP] = 60 μM, (■) E441Q, [(*E*)-FMCDP] = 60 μM; and (○) C225S, [(*Z*)-FMCDP] = 60 μM.

Interaction of (E)-FMCDP with E441QR1. The failure to detect a substantial decrease in radiolabeling of the C→S mutants suggested that E441 could be the residue that is alkylated. Previous crystallographic studies have revealed that it is located within the active site of R1, and modeling studies suggested that it is located on the α-face of the nucleotide (Uhlin & Eklund, 1994). As studies with the mutant E441QR1 have not been previously reported, it was initially characterized with the normal substrate. E441QR1 catalyzed the turnover of 12 equiv of CDP prior to its complete inactivation. During this time about 34% of the tyrosyl radical was reduced. Characterization of the products of the reaction showed the production of four dCDPs and eight cytosines. The initial rate of dCDP formation was determined to be 22 nmol min^{-1} mg^{-1}, corresponding to 1.6% of wt activity. Previous studies have shown the presence of about 1−3% of contaminating wt-R1 in preparations of R1 mutants expressed in *E. coli* (Mao et al., 1992b). The quantities of dCDP detected in the present studies can therefore be attributed to wt-R1. On the other hand, the cytosine is produced by E441QR1, indicating it can catalyze 3′ hydrogen atom abstraction from the nucleotide.[4] In experiments in which TR, TRR, and NADPH were present as a reducing system, formation of a chromophore at 317 nm was detected accompanying inactivation similar to observations during previous studies on the interaction of C225S and C462S with CDP (Mao et al., 1992a,b). The fact that E441QR1 can catalyze 3′ carbon−hydrogen bond cleavage resulting in cytosine production suggested that its analysis with FMCDP could be profitable.

Very different results were obtained during the interaction of E441QR1 with (*E*)-FMCDP in comparison with the cysteine mutants. Incubation of this mutant with [6′-^{14}C-]-(*E*)-FMCDP for 3 h resulted in only 0.24 label per R1, release of 1.4 equiv of cytosine, and reduction of 45% of the tyrosyl radical. Furthermore, instead of the absorbance at 334 nm, a broad absorbance with weak intensity at 317 nm was observed. These results thus suggest that the observed covalent modification (0.24 label/R1) could result from furanone-like alkylation and that E441 is a likely candidate for the stoichiometric labeling of wt-R1.

DISCUSSION

(*E*)- and (*Z*)-FMCDP are very effective inhibitors of RDPR, inactivating both of its subunits (Figures 1 and 2). The observation that inactivation is more rapid than tyrosyl radical loss requires that both R1 alkylation and R2 reduction ($Y^{\bullet}$ loss) are responsible for inactivation. (*E*)- and (*Z*)-FMCDP showed very similar ratios of turnovers per inactivation event (∼1.4) and similar chemistries, including fluoride release, cytosine formation, tyrosyl radical loss, generation of a new radical, and chromophore formation (Figures 1−4 and Table 1). In the case of all nucleotide inhibitors examined thus far, and these are no exception, the reductant (DTT or TR/TRR/NADPH) alters the relative partitioning between the various modes of inactivation. These results are particularly interesting, given that only (*E*)-FMC appears to be clinically active (McCarthy & Sunkara, 1995), and suggest that the metabolism of the two isomers might be different *in vivo*.

Mechanism of Inactivation. A working hypothesis to accommodate the available data is shown in Schemes 2 and 3 and is based on previous studies of the mechanism based inhibitors ClUDP and N_3UDP (Scheme 1). Inactivation is initiated by 3′ hydrogen atom abstraction by thiyl radical C439. Homolytic scission of the 3′ carbon-hydrogen bond would produce an allylic radical **3** (Scheme 2). This intermediate can then be reduced, as per the paradigm in Scheme 1, from the top face via C439 or the bottom face via C225 or C462 to produce **4**. Reduction from the top face regenerates the thiyl radical and hence $Y^{\bullet}$ (minor pathway, Scheme 2), while reduction from the bottom face leads to $Y^{\bullet}$ loss (major pathway, Scheme 2), the predominant mechanism of inactivation of RDPR by these inhibitors. Intermediate **4** can rapidly lose fluoride to give **5** containing an exocyclic methylene conjugated to a ketone which is highly activated toward nucleophilic attack. Such an attack by a protein residue (Scheme 3, pathway A) could account for R1 inactivation, the observed covalent modification of the enzyme (∼1 equiv/R1), the slow loss of cytosine from this initial adduct under native conditions, and its rapid loss under denaturing conditions.[5]

The rapid release of 0.5 cytosine, in the presence or absence of DTT, could result from **5** dissociating from the active site and decomposing in solution to release cytosine concomitant with trapping by DTT or nonspecific alkylation of R1 (Scheme 3, pathway B). At this stage it is not clear whether the formation of the 334 nm chromophore on R1 is associated with pathway A or B (Scheme 3). Studies with DTT present during the inactivation event were initially

[4] While not analyzed in detail, E441DR1 does catalyze dCDP formation at 5−6% the rate of wt-R1, indicating that E441 is not essential for catalysis.

[5] It should be pointed out that while R1 and R2 are each composed of two identical polypeptides, there is only one tyrosyl radical, not two, per R2. Since this radical is essential for catalysis, its destruction results in inactivation of RDPR even though only one of the two active sites on R1 is modified.

Scheme 2

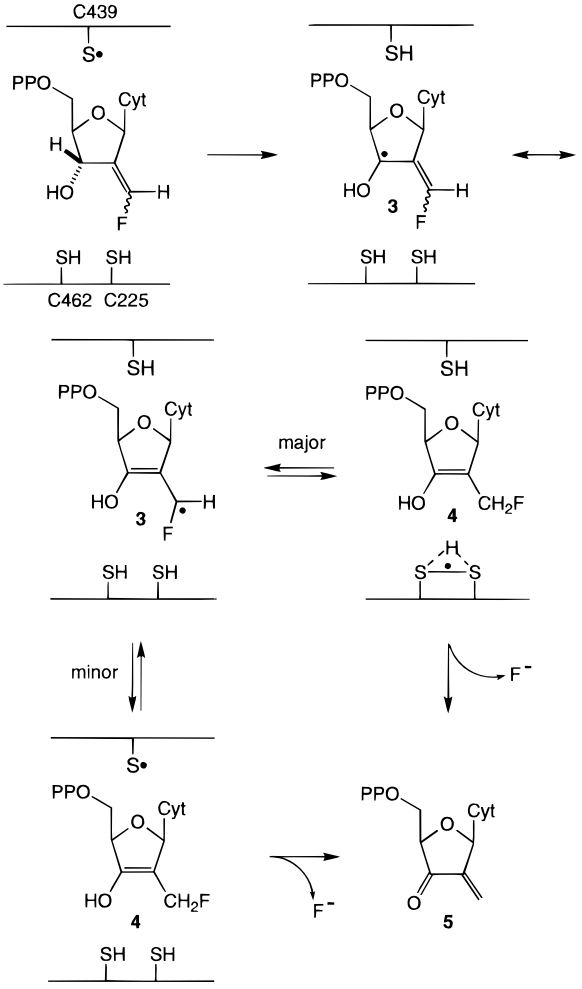

Scheme 3

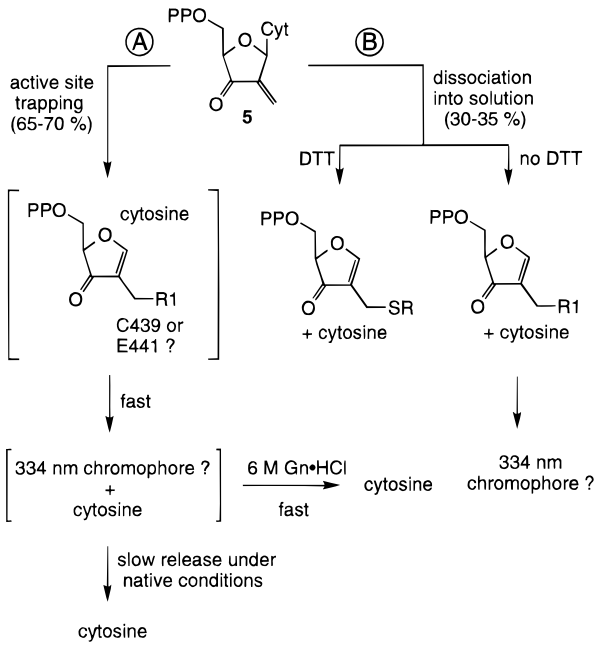

carried out to address this question. Specifically, if the solution pathway (Scheme 3, pathway B) was responsible for the observed chromophore, then DTT could trap this species and prevent its formation. However, studies with a variety of mechanism-based inhibitors indicate that reductant

Scheme 4

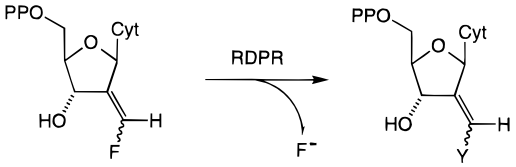

(DTT, TR, TRR, etc.) can change the partitioning of intermediates leading to inactivation. Thus, while DTT did prevent chromophore formation and 0.3 equiv of radiolabeling consistent with trapping in solution, it could do so by more than one mechanism.

In addition to the inactivation mechanism discussed above an alternative explanation for the experimental observations must also be considered. The groups of McCarthy and Borchardt have previously studied the inactivation of *S*-adenosyl-L-homocysteine (AdoHcy) hydrolase by (*Z*)-4′,5′-didehydro-5′-deoxy-5′-fluoroadenosine (ZDDFA) (McCarthy et al., 1989; Mehdi et al., 1990; Yuan et al., 1993). AdoHcy hydrolase requires enzyme-bound NAD^+ for the hydrolysis of its natural substrate. The function of this cofactor is to oxidize the 3′-hydroxyl of AdoHcy to a ketone, facilitating the elimination of homocysteine to form an α,β-unsaturated adenosine derivative (Palmer & Abeles, 1979). Addition of H_2O to this α,β-unsaturated ketone followed by re-reduction of the 3′-ketone then produces adenosine and regenerates NAD^+. Surprisingly, it was found that the apo-enzyme (no enzyme-bound NAD^+ or NADH) was capable of catalyzing the conversion of ZDDFA to adenosine-5′-carboxaldehyde concomitant with fluoride release (Yuan et al., 1993). This unusual result suggests that the active site environment of the enzyme can activate the exocyclic fluoromethylene group of the nucleoside toward nucleophilic addition by a water molecule without prior oxidation of the 3′-hydroxyl. After the addition of the water, the carboxaldehyde is produced by elimination of fluoride ion. In the case of FMCDP a similar addition/elimination reaction sequence involving a protein nucleophile can be envisaged, and this could account for both the observed release of fluoride and the stoichiometric radiolabeling of a protein residue (Scheme 4).[6] No fluoride release or radiolabeling was observed in experiments where met-R2 replaces wt-R2. Thus, if this mechanism pertains, generation of the thiyl radical on C439 or 3′ hydrogen abstraction must be required for the addition/elimination process. A distinction between these mechanistic possibilities (Schemes 2−4) might be assisted by structural characterization of the new radical species detected by EPR spectroscopy. These, and other studies, are presently in progress.

Studies with N_3UDP and ClNDPs have revealed chromophore formation at 320 nm. Model studies have previously provided a satisfactory chemical explanation for these chromophores (Ashley et al., 1988). A red-shift of 10 nm would be predicted for the chromophore formed with FMCDP on the basis of the additional methylene substituent (Woodward, 1942). Thus, the experimentally observed red-shift of 14 nm is consistent with a chemical structure similar

[6] We were unable to find chemical precedent for this reaction and FMCDP is stable to thiolates at pH 9. Thus, if this mechanism pertains, the active site would have to enhance the reactivity of the exocyclic fluorinated methylene group.

to that proposed for the chromophore produced with N_3UDP and ClNDPs. However, the much faster rate of formation of the chromophore with FMCDP (Figure 4) compared with studies on N_3UDP and ClNDP is not readily explained with the previous hypothesis. Therefore solid state NMR studies with labeled FMCDP are in progress in an effort to define the structure associated with this chromophore.

The stoichiometric labeling of R1 raised hopes that an active site residue was involved and could be identified by peptide mapping. Unfortunately all efforts failed to isolate a labeled peptide and in the traces from the HPLC chromatographic analysis, extensive scrambling of the label was detected. To further address the residue involved in trapping the putative intermediate **5** (Scheme 3), the interaction of FMCDP with a variety of site-directed mutants, including C462S, C225S, and C754/759S, was investigated. With these mutants covalent modification of R1 still resulted, although the partition ratios between the mechanisms contributing to the inactivation appear to have been altered. C439 and E441 are also within the active site and hence are viable candidates for modification. The results with E441QR1, only 0.2 equiv of radiolabel per R1 and no chromophore at 334 nm, suggest that glutamate 441 is a reasonable candidate for the alkylated residue. If the mechanism in Schemes 2 and 3 pertains, then the possible involvement of C439 cannot be tested using site-directed mutagenesis, as C439 is essential for 3′ hydrogen atom abstraction required to initiate the inactivation event. If the mechanism in Scheme 4 pertains, one might have expected that C439SR1 would be radiolabeled which is not observed. Thus, it is likely that 3′ hydrogen abstraction is in fact required for the inactivation event in both models. C439 therefore remains a candidate for alkylation by FMCDP. Studies of Kyte and co-workers (1987) suggest that an antibody raised to a peptide containing cysteine 439 and/or glutamate 441 might allow successful purification of a potentially modified peptide at neutral pH. These studies are in progress.

Finally, the mechanism in Scheme 2 predicts that an allylic radical is generated concomitant with tyrosyl radical loss, and preliminary results suggests that the new radical species detected (Figure 3) is substrate derived. Experiments using isotopically labeled FMCDP and high-frequency EPR (140 GHz) are in progress to further characterize this species.

SUMMARY

These studies of the interaction of (*E*)-FMCDP with RDPR from *E. coli* show that it is a potent mechanism-based inhibitor of the enzyme. Preliminary results indicate that this nucleotide analog also potently inactivates mammalian RDPR from mouse. Thus, these observations suggest that the *in vivo* cytotoxicity of the parent nucleoside in tumor cells could be a consequence of the inhibition of both RDPR and DNA polymerase potentiating the suppression of DNA biosynthesis.

SUPPORTING INFORMATION AVAILABLE

Descriptions of RDPR inactivation with (*Z*)- and [6′-^{14}C]-(*E*)-FMCDP and of treatment of the inactivated protein with NaB^3H_4 before and with $NaBH_4$ after denaturation (2 pages). Ordering information is given on any current masthead page.

REFERENCES

Abbruzzese, J. L., Grunewald, R., Weeks, E. A., Gravel, D., Adams, T., Nowak, B., Mineishi, S., Tarasoff, P., Satterlee, W., Raber, M. N., & Plunkett, W. (1991) *J. Clin. Oncol. 9*, 491−498.

Åberg, A., Hahne, S., Karlsson, M., Larrson, Å., Ormö, M., Åhgren, A., & Sjöberg, B. M. (1989) *J. Biol. Chem. 264*, 2249−2252.

Ashley, G. W., Harris, G., & Stubbe, J. (1988) *Biochemistry 27*, 4305−4310.

Ator, M. A., & Stubbe, J. (1985) *Biochemistry 24*, 7214−7221.

Ator, M., Salowe, S. P., Stubbe, J., Emptage, M. H., & Robins, M. J. (1984) *J. Am. Chem. Soc. 106*, 1886−1887.

Baker, C. H., Banzon, J., Bollinger, J. M., Jr., Stubbe, J., Samano, V., Robins, M.J., Lippert, B., Jarvi, E., & Resvick, R. (1991) *J. Med. Chem. 34*, 1879−1884.

Berglund, O., & Eckstein, F. (1974) *Methods Enzymol. 34B*, 253−261.

Bianchi, V., Borella, S., Calderazzo, F., Ferraro, P., Chieco Bianchi, L., & Reichard, P. (1994) *Proc. Natl. Acad. Sci. U.S.A. 91*, 8403−8407.

Bollinger, J. M., Jr., Edmonson, D. E., Huynh, B. H., Filley, J., Norton, J. R., & Stubbe, J. (1991) *Science 253*, 292−298.

Ellis, M. N., Lobe, D. C., & Spector, T. (1989) *Antimicrob. Agents Chemother. 33*, 1691−1696.

Eriksson, S., & Sjöberg, B. M. (1989) *Allosteric Enzymes* (Hervé, G., Ed.) CRC, Boca Raton, FL.

Gao, W.-Y., Cara, A., Gallo, R. C., & Lori, F. (1993) *Proc. Natl. Acad. Sci. U.S.A. 90*, 8925−8928.

Grunewald, R., Du, M., Adams, T., Faucher, K., Kantarjian, H., Keating, M., Tarasoff, P., Raber, M., & Plunkett, M. (1990) *Proc. Am. Assoc. Cancer Res. 31*, 182.

Harris, G., Ator, M., & Stubbe, J. (1984) *Biochemistry 23*, 5214−5225.

Hoard, D. E., & Ott, D. G. (1965) *J. Am. Chem. Soc. 87*, 1785−1788.

Huang, P., Chubb, S., Hertel, L. W., Grindey, G. B., & Plunkett, W. (1991) *Cancer Res. 51*, 6110−6117.

Kanazawa, J., Kakahashi, T., Gomi, K., & Okabe, M. (1995) *Proc. Am. Assoc. Cancer Res. 36*, 405.

Karlsson, A., & Harmenberg, J. (1988) *Antimicrob. Agents Chemother. 32*, 1100−1102.

Kyte, J., Xu, K.-Y., & Bayer, R. (1987) *Biochemistry 26*, 8350−8360.

Lin, A. I., Ashley, G. W., & Stubbe, J. (1987) *Biochemistry 26*, 6905−6909.

Lori, F., Malykh, A., Cara, A., Sun, D., Weinstein, J. N., Lisziewicz, J., & Gallo, R. C. (1994) *Science 266*, 801−805.

Lunn, C. A., Kathju, S., Wallace, B. J., Kushner, S., & Pigiet, V. (1984) *J. Biol. Chem. 259*, 10469−10474.

Malmström, B., Reinhammar, B., & Vänngård, T. (1970) *Biochim. Biophys. Acta 205*, 48.

Mao, S. S., Johnston, M. I., Bollinger, J. M., Jr., & Stubbe, J. (1989) *Proc. Natl. Acad. Sci. U.S.A. 86*, 1485−1489.

Mao, S. S., Holler, T. P., Bollinger, J. M., Jr., Yu, G. X., Johnston, M. I., & Stubbe, J. (1992a) *Biochemistry 31*, 9744−9751.

Mao, S. S., Holler, T. P., Yu, G. X., Bollinger, J. M., Jr., Booker, S., Johnston, M. I., & Stubbe, J. (1992b) *Biochemistry 31*, 9733−9743.

Mao, S. S., Yu, G. X., Chalfoun, D., & Stubbe, J. (1992c) *Biochemistry 31*, 9752−9759.

Matthews, D. P., Persichetti, R. A., Sabol, J. S., Stewart, K. T., & McCarthy, J. R. (1993) *Nucleosides Nucleotides 12*, 115−123.

McCarthy, J. R., Jarvi, E. T., Matthews, D. P., Edwards, M. L., Prakash, N. J., Bowlin, T. L., Mehdi, S., Sunkara, P. S., Bey, P. (1989) *J. Am. Chem. Soc. 111*, 1127−1128.

McCarthy, J. R., Matthews, D. P., Stemerick, D. M., Huber, E. W., Bey, P., Lippert, B. J., Snyder, R. D., & Sunkara, P. S. (1991) *J. Am. Chem. Soc. 113*, 7439−7440.

McCarthy, J. R., & Sunkara, P. S. (1995) *Chemical and Structural Approaches to Rational Drug Design* (Weiner, D. B., & Williams, W. B., Eds.) CRC Press, Boca Raton, FL.

Mehdi, S., Jarvi, E. T., Koshi, J. R., McCarthy, J. R., Bey, P. (1990) *J. Enzyme Inhib. 4*, 1−13.

Palmer, J. L., & Abeles, R. H. (1979) *J. Biol. Chem. 254*, 1217−1226.

Reichard, P. (1993) *Science 260*, 1773−1777.
Russel, M., & Model, P. (1985) *J. Bacteriol. 163*, 238−242.
Salowe, S. P., & Stubbe, J. (1986) *J. Bacteriol. 165*, 363−366.
Salowe, S. P., Ator, M., & Stubbe, J. (1987) *Biochemistry 26*, 3408−3416.
Salowe, S. P., Bollinger, J. M., Jr., Ator, M., Stubbe, J., McCracken, J., Peisach, J., Samano, M. C., & Robins, M. J. (1993) *Biochemistry 32*, 12749−12760.
Sjöberg, B.-M., Reichard, P., Gräslund, A., & Ehrenberg, A. (1977) *J. Biol. Chem. 252*, 536−541.
Sjöberg, B.-M., Gräslund, A., & Eckstein, F. (1983) *J. Biol. Chem. 258*, 8060−8067.
Spector, T., Averett, D. R., Nelson, D. J., Lambe, C. U., Morrison, R. W., Jr., St.Clair, M. H., & Furman, P. A. (1985) *Proc. Natl. Acad. Sci. U.S.A. 82*, 4254−4257.
Steeper, J. R., & Steuart, C. D. (1970) *Anal. Biochem. 34*, 123−130.
Stubbe, J. (1990a) *J. Biol. Chem. 265*, 5329−5332.
Stubbe, J. (1990b) *Adv. Enzymol. Relat. Areas Mol. Biol. 63*, 349−417.
Stubbe, J., & Kozarich, J. W. (1980a) *J. Biol. Chem. 255*, 5511−5513.
Stubbe, J., & Kozarich, J. W. (1980b) *J. Am. Chem. Soc. 102*, 2505−2507.
Thelander, L., Larsson, B., Hobbs, J., & Eckstein, F. (1976) *J. Biol. Chem. 251*, 1398−1405.
Uhlin, U., & Eklund, H. (1994) *Nature 370*, 533−539.
van der Donk, W. A., Stubbe, J., Gerfen, G. J., Bellew, B. F., & Griffin, R. G. (1995) *J. Am. Chem. Soc. 117*, 8908−8916.
Woodward, R. B. (1942) *J. Am. Chem. Soc. 62*, 76−77.
Yoshikawa, M., Kato, T., & Takenishi, T. (1967) *Tetrahedron Lett. 50*, 5065−5068.
Yuan, C.-S., Yeh, J., Liu, S., Borchardt, R. T. (1993) *J. Biol. Chem. 268*, 17030−17037.

BI960190J